Reeves, et al., J. Geophys. Res., 97, 6417, 1992.

Further Investigation of the CDAW 7 Substorm Using Geosynchronous Particle Data: Multiple Injections and Their Implications

G. D. REEVES, G. KETTMANN, T. A. FRITZ, AND R. D. BELIAN
Los Alamos National Laboratory, Los Alamos, New Mexico

A substorm which occurred on April 24, 1979 was the subject of the CDAW 7 workshop and several in-depth studies of ISEE and ground-based data. In this paper we continue the analysis by looking in detail at geosynchronous energetic particle data from the Los Alamos charged particle analyzer instruments. Observations show three distinct injection events during this substorm. We have used a drift shell tracing technique to determine the time and location on the geosynchronous drift shell of each injection region. We then compare the timing of events on the ground, in the tail and at geosynchronous orbit. The first injection is very closely associated with observations from ISEE and ground-based measurements which have been interpreted as the signatures of plasmoid formation in the near-Earth tail. The later two injections occurred while ISEE 1 and 2 were in the lobes following the exit of the plasmoid downtail. All three injections are calculated to have originated in the same local time sector in which the ISEE spacecraft were located and also to have overlapped one another in local time extent. These observations show that the spatial and temporal evolution of the substorm is more dynamic than previous studies have implied. We have considered possible interpretations of the more complete set of observations the context of the both the traditional near-Earth neutral line model and the inner magnetospheric current disruption model. Either model can provide an interpretation of the data but neither by itself, provides a completely satisfactory explanation. We suggest a new synthesis of these two models which provides a simple interpretation for all the observations. We propose that reconnection in the tail initiates the substorm but diverts much of the cross-tail current around the reconnection region enhancing the near-Earth cross-tail current. This creates an unstable situation and current disruptions dipolarize the field in three steps creating the three injections.

INTRODUCTION

The most widely adopted model of magnetospheric substorms is the near-Earth neutral line, or plasmoid, model [e.g., *McPherron et al.*, 1973; *Hones*, 1979]. In this model, flux is added to the magnetotail lobes by reconnection on the dayside of the magnetosphere and subsequent transport of the reconnected field lines, by solar wind flow, into the magnetotail. Currents in the plasma sheet distort the tail magnetic field lines, stretching them antisunward. At some critical point, field lines in the tail reconnect forming the so-called "near-Earth neutral line" or "*X* line." Current is diverted into the ionosphere creating the substorm current wedge [*McPherron et al.,* 1973], and particles are precipitated causing a brightening of the aurora. Reconnected field lines still attached to the Earth snap back to a more dipolar configuration and transport plasma earthward creating the substorm injections commonly observed in the vicinity of geosynchronous orbit. Reconnection continues forming a bubble of plasma on *O*-type field lines referred to as a plasmoid. Reconnection in the central and boundary plasma sheet may continue until the last closed tail field line reconnects: at this point open, lobe field lines begin reconnecting and the severed plasmoid accelerates antisunward. This process redistributes much of the energy which has been loaded into the magnetotail and returns the magnetosphere to a more relaxed configuration while the plasmoid continues off into interplanetary space with the solar wind.

This qualitative picture has provided a conceptual framework for decades, but recent attempts to investigate, quantitatively, the relationship between different pieces of the overall process have cast doubt upon this model. As an example, there is not consensus on the location of initiation of the substorm. G. Kettmann et al. (Energetic Ion Anisotropies in the Geomagnetic Tail: 1. A Statistical Survey, submitted to *Journal of Geophysical Research*) found through a statistical analysis of ISEE data that although strong earthward energetic ion anisotropies were considerably more frequently observed, strong tailward directed ion streaming presumably associated with reconnection earthward of the ISEE spacecraft was occasionally detected tailward of $X \approx 16\ R_E$, with the probability of observing such an event increasing with downtail distance. They concluded that the neutral line sometimes formed inside the ISEE orbit (i.e., inside $X \approx 23\ R_E$) In contrast, *Baumjohann et al.* [1989, 1990], using data from the active magnetospheric particle tracer explorer ion release module (AMPTE/IRM), found that the high-speed tailward flows expected tailward of the reconnection region are rarely if ever located inside about 19 R_E. There have been also studies that suggest that substorm reconnection may begin earthward of 10 R_E [e.g., *Fritz et al., 1984; Baker et al.*, 1982]. There is certainly evidence of substantial deformation of the

magnetic field at geosynchronous orbit at 6.6 R_E [e.g., *Kaufmann*, 1987 and references therein].

Questions raised by these and other observations (many of which represent dramatic improvements in time resolution, energy resolution, and spatial coverage over the observations which formed the basis of the plasmoid model) have led some researchers to propose significant extensions to the original plasmoid model and have led other researchers to propose alternative mechanisms for producing substorms. A substorm which occurred on April 24, 1979 has received considerable attention in this debate. This event was a subject of study in the seventh Coordinated Data Analysis Workshop (CDAW 7). It was originally interpreted as strongly supporting the plasmoid substorm model [*Hones et al.*, 1986]. *Eastman et al*. [1988] argued that the magnetic field changes and plasma and energetic particle measurements at ISEE-1 and-2 were equally consistent with the plasma sheet boundary layer (PSBL) model and could be interpreted within that context. For example, southward motion of the northern plasma sheet boundary layer could be interpreted as thinning of the plasma sheet or as motion of the plasma sheet as a whole. *Kettmann et al.* [1990] reexamined the ISEE energetic particle data. They found that, while prior to substorm onset the motion of the plasma sheet boundary layer was as described, following substorm onset a layer of strongly tailward flows which did not previously exist was detected below the ISEE-2 spacecraft. The motion of this flow layer was from the central plasma sheet toward the lobe which was interpreted as the expansion of the plasmoid separatrix layer. Their detailed analysis strongly supports the interpretation that a plasmoid was formed and provides very accurate timing of important stages in the substorm process.

In other substorm models the existence of a plasmoid does not imply that the formation of a near-Earth reconnection region causes the substorm. Rather, they suggest that the formation of a near-Earth reconnection region and the production of a plasmoid may be one of the consequences of some other substorm onset process which occurs at some earlier time. One such model has come to be known as the current sheet disruption model [e.g., *Takahashi et al.,* 1987; *Lui et al*., 1988; *Lopez et al*., 1988, 1990; *Lopez and Lui*, 1990]. In this model, strong currents in the nightside of the inner magnetosphere ($R < 10\ R_E$) are disrupted (by one of a number of possible mechanisms other than reconnection) and diverted into the ionosphere, likewise producing a substorm current wedge and visible aurorae. The current disruption is directly responsible for the energization of plasma producing a substorm injection. The current disruption region is envisioned to expand radially and azimuthally in either piecewise or continuous fashion [*Lopez et al.,* 1990] and could, if conditions favor it, produce a near-Earth reconnection region sometime after onset.

None of the previous studies of this event considered the substorm signatures observed at geosynchronous orbit. In this paper we extend the analysis of the CDAW 7 substorm by investigating energetic particle measurements at geosynchronous orbit and comparing those results to ground-based and ISEE 1 and 2 measurements. In our analysis we adopt the interpretation of *Hones et al.* [1986] and *Kettmann et al.* [1990] that a plasmoid was formed in the near-Earth magnetotail and investigate what more the geosynchronous observations can disclose concerning important substorm processes. Since the current sheet disruption model contains an explicit mechanism for producing particle signatures at geosynchronous distances, we consider whether the CDAW 7 substorm can be interpreted within this context. We also consider what the geosynchronous energetic particle observations imply for the actual injection mechanisms in the near-Earth neutral line and current disruption models.

INSTRUMENTS AND MEASUREMENTS

The Los Alamos charged particle analyzer (CPA) instruments have been operated at geosynchronous orbit continuously since 1976. Up to four spacecraft are in operation simultaneously to provide a global monitoring capability. During the CDAW 7 substorm, Los Alamos instruments were on board two geosynchronous spacecraft: 1977-007 and 1976-059. Spacecraft 1976-059 experienced an untimely loss of data during the early portion of the substorm and will not be included in this analysis. The CPA instruments are capable of measuring electrons in the energy range 30 keV to 1.5 MeV and ions with energies from 90 keV to 220 MeV. Protons are measured in the equatorial plane of each spacecraft every 256 ms with two sets of detectors. (The spin axis points toward the Earth.) The LoP detector monitors protons with 10 integral energy channels with lower thresholds between ≈90 and ≈300 keV and a common high energy threshold of ≈ 600 keV. The HiP detector measures protons with 16 differential energy channels from ≈0.4 to ≈150 MeV. Energetic electrons are also measured in the spacecraft equatorial plane by the HiE detector with six integral channels in the energy range 0.2 to 1.5 MeV. Electrons in the energy range 30 to 300 keV are measured in six energy channels by the LoE detector. The LoE instrument consists of a set of five detectors mounted at angles of 0°, ±30°, and ±60°. None of these spacecraft is equipped with a magnetometer. More complete descriptions of the CPA instruments can be found in the works by *Higbie et al.* [1978], *Belian et al.* [1978], and *Baker et al.* [1979].

ISEE results referred to in this paper were obtained primarily with two instruments. The Medium Energy Particle Experiment (MEPE) which measures both ions in the energy

range of about 25 to 2500 keV and electrons from 20 to 1200 keV has been thoroughly described by *Williams et al.* [1978]. The magnetometer characteristics and capabilities are presented by *Russell* [1978].

GROUND-BASED MAGNETIC OBSERVATIONS

Magnetograms from April 24, 1979 show clear evidence of the CDAW-7 substorm but are less clear on the exact time of substorm onset. *Hones et al.* [1986] place at onset at 1112 UT based primarily on the *H* components from College (Figure 1) and Honolulu. *Eastman et al.* [1988] using the same data place onset at 1111 UT ± 1 min. Pushing the resolution of the data, one can note that the initial change in slope indicating magnetic perturbation actually began closer to 1110 UT (which is marked in Figures 1 and 2 with a dotted line). The discrepancy arises from using different criteria for "onset." The magnetogram from Cape Wellen (which was not discussed in any earlier studies of this event) also shows changes in the *D* and *Z* components of the magnetic field at approximately 1110 UT (Figure 2). A gradual decrease in the *H* component began somewhat earlier at 1107 UT and steadily intensified until approximately 1118 UT. (Note that Figures 1 and 2 were reproduced for publication purposes, whereas all timing was obtained from photocopies of the original magnetograms but can be considered accurate only to about ±1 min.)

A clear signature of the beginning of recovery is even more difficult to pin down than the onset of activity. However, it is clear that significant ionospheric current intensifications occurred until at least 1140 UT. Three times, 1114, 1118, and 1135 UT, are indicated in Figures 1 and 2 with thin solid lines. These times correspond to the onset times for geosynchronous energetic particle injections as will be discussed in a later section. Here we note that these times also correspond to changes in the ionospheric currents. At College, all three times correspond closely to decreases in the magnitude of all three components of the field. At Cape Wellen, on the other hand, the *Z* component shows no dramatic excursions from its gradual diminution while at approximately 1118 and 1135 UT the *H* and *D* components increase. Cape Wellen shows only marginally observable variations at 1114 UT. It can also be noted that the *H* and *D* components at Cape Wellen show additional increases at approximately 1121 UT, while at College at this time the three components show no simultaneous changes but are generally returning toward their nominal values. For reference, we note the geographic locations of the two auroral stations: Cape Wellen at 66° latitude and 170° longitude and College further to the east at 65° latitude and 212° (or -148°) longitude.

The ground magnetic field perturbations are also reflected in the *AE* and *AL* indices which are shown in Figure 3. Again, we have marked 1110 UT and 1114, 1118, and 1135 UT for later comparison. By this measure the substorm intensity begins to build around 1110 UT and continues to increase to a maximum between 1134 and 1135 UT. Thereafter the intensity measured by *AE* and *AL* decreases.

A REVIEW OF ISEE OBSERVATIONS

Prior to substorm onset, ISEE 1 and 2 were in the plasma sheet at approximately 21 R_E down the tail (geocentric distance), 5 R_E duskward of the midnight meridian, and 0.8 R_E above the nominal position of the neutral sheet. ISEE 2 was somewhat earthward of ISEE 1 and closer to the neutral sheet, south of ISEE 1. *Kettmann et al.* [1990] used a remote sensing method to probe flux boundaries within an ion gyrodiameter of the ISEE spacecraft [e.g., *Andrews et al.*, 1981; *Daly and Keppler*, 1983]. They found that, prior to substorm onset, ISEE 1 and 2 were inside the central plasma sheet, within a few ion gyroradii of the northern lobe and measured the inward contraction speed to be about 10 km/s [*Kettmann et al.,* 1990].

The onset of overall flux increases as measured by the ISEE 2 plasma analyzer began just prior to 1112 UT [*Hones et al.*, 1986]. Corresponding energetic particle flux increases were reported by *Kettmann et al.* [1990] beginning at 1112:10 UT. Strong tailward streaming was first observed at ISEE 2 at 1113:00 UT and continued up to ≈1117 UT [*Kettmann et al.*, 1990]. From the pitch angle distributions, *Kettmann et al.* [1990] determined that the tailward ion flows starting at 1113:00 UT were located south of the spacecraft. By 1113:16 the majority of streaming ions had a pitch angle of 180° and tailward streaming ions north of ISEE 2 appeared. It is apparent that a layer of strong tailward flowing ions was created within the plasma sheet and subsequently expanded north across the location of ISEE 2. *Kettmann et al.* [1990] interpreted this as the separatrix layer mapping to the reconnection region earthward of the spacecraft.

ISEE 1 also sensed the separatrix layer to the south of its location, but its appearance was delayed approximately 30 s with respect to observations at ISEE 2 again indicating northward motion of the flow layer. Since ISEE 1 never measured strong tailward flows with gyrocenters north of the spacecraft, one can conclude that the separatrix layer never passed over the location of ISEE 1 but rather, paused between ISEE 1 and ISEE 2. At 1115:20, ISEE 2 was on open field lines and the plasmoid exited downtail [*Kettmann et al.*, 1990]. From ≈1116 to ≈1141 UT the ion plasma pressure at ISEE 2 was below detector thresholds with the exception of a brief interval at ≈1125 UT when ISEE 2 reencountered a

region of measurable ion plasma pressure [*Hones et al.,* 1986] and tailward streaming energetic ions [*Kettmann et al.,* 1990]. Thus the ISEE spacecraft were sensitive to plasma sheet processes near the onset of the substorm but generally remained in the lobes for the duration of the substorm.

GEOSYNCHRONOUS OBSERVATIONS AND ANALYSIS

Spacecraft 1977-007 was located at -133.3° geographic longitude. Therefore the local time is equal to UT-8.89 hour which put the spacecraft about 2.3 hours east of midnight at substorm onset. Hence it was well located to observe the electron signature of the injection (Figure 4). The data are spin averaged (10.8 s) and averaged over five look directions and therefore average over all pitch angles. The absolute flux levels are unimportant for this analysis so the curves in Figure 4 for various energies are offset so that their shape can be seen more clearly. In Figure 5 the 65-95 keV flux curve is replotted on a linear scale to highlight the important features. This injection is somewhat complex but also very interesting — especially in the context of the picture of the substorm painted by the ISEE data. A weak growth phase decrease in particle fluxes preceded the injection [*McPherron,* 1970; *Baker et al.,* 1978, 1984]. The end of the weak growth phase decrease (determined by a change in sign of the derivative of the flux) occurred at 1112 UT ± 1 min in all energy channels. The substorm injection raised fluxes to above the levels which existed prior to the growth phase. In the lowest energy channels, fluxes increased by nearly an order of magnitude.

Superimposed upon the broad injection feature are three distinct injection peaks which are seen to be dispersed in energy. At higher energies, all peaks are seen as distinct, separate features while at lower energies the first two peaks are more dispersed and partially overlap. Such small, impulsive injections within the overall substorm injection are not rare. They have been discussed by *Belian et al.* [1984] and, more recently, by *Yahnin et al.* [1990]. Multiple onsets of activity within a substorm are also seen in geosynchronous magnetic field data [e.g., *Nagai et al.,* 1983], from ground-based magnetograms [e.g., *Wiens and Rostoker*, 1980], and from ISEE 3 measurements in the deep tail [*Slavin et al.,* 1984].

Dispersion in the onset of the injection pulse for different energy bands implies that spacecraft 1977-007 was located east of the substorm injection region. This complicates a comparison of ISEE and geosynchronous data since the time at which 1977-007 saw an injection feature is the time at which that feature appeared on the geosynchronous drift shell plus the time it took the particles to drift to the spacecraft. We can facilitate the analysis by calculating the time and location at which these features appeared on the drift shell at 6.6 R_E.

We have used a drift shell tracing technique [*Reeves et al.,* 1990, 1991] to remove the effect of the drift from the injection region to the spacecraft. The essence of this technique involves calculating the bounce-averaged gradient and curvature drift velocity of trapped particles at all local times along the drift shell and projecting the observed injection signatures backward along the drift shell to their point of injection. The drift shell is calculated by numerically solving for the locus of field lines (in a particular model field) on which the first two adiabatic invariants are conserved. In this analysis we use the field model of *Tsyganenko and Usmanov* [1982]. The drift velocities for electrons and protons of all detected energies are calculated by numerically solving the equation of motion for the bounce average drift velocity:

$$V_D \equiv \langle V_{GC} \rangle = \frac{2\pi E}{q S_b B_0} \nabla_0 I \times \hat{\mathbf{B}}_0,$$

where V_{GC} is the gradient-curvature drift velocity, E is the kinetic energy, S_b is the so-called half-bounce path length, $\nabla_0 I$ is the gradient of the invariant integral, and the subscript 0 denotes values at the magnetic equator [*Roederer,* 1970].

A representative projection plot is shown in Figure 6. The time and location at which the peak was observed in each energy channel is plotted at the upper right of the figure. Particle trajectories are traced backward along the drift shell (down and left) through a 360° drift. The point at which lines for all energies converge defines the time and location of the injection of this feature. In this case, peak 2 originated on the drift shell at 1118:00 UT, 1° west of midnight (-1° in the figure). Because of the short distance through which the electrons had to drift, the convergence of lines for different energies is quite good and the injection point is well defined. This analysis was repeated for the other two peaks and the onset of the injection (projections not shown).

The results are shown in Figure 7. The onset of the electron injection flux increases are observed between 1114 and 1120 UT for different energies (Figure 4). The observed injection onset is produced by the first particles to drift from the injection region to the spacecraft, and therefore it projects back to the easternmost edge of the injection region which was located at 21.5° east of midnight and is labeled "Electron Edge" in Figure 7. The injection of electrons on the drift shell at that location occurred at 1113:48 (all projected injection times are ±30 s). The first peak also has an injection time of 1113:48 but is located at 10.0°, somewhat further west than the edge of onset. The second peak was injected onto the drift shell at 1118:00 at -1° from local midnight, and the third peak was injected at 1134:48 at 0°.

It is important to realize that the projection of the peaks in the electron flux do not define the center of the injection region but rather a point near its eastern edge. This is known from

previous studies (e.g., *Reeves et al.* [1990, 1991]) which show that the electron and ion peaks do not project to the same point. The electron peaks project to points near the "electron edge," and the ion peaks project to points near the "ion edge." The electron and ion "edges" are defined by the first particles to arrive at the spacecraft and therefore the easternmost and westernmost extents of the injection region. One reason the peaks do not project to the center of the injection region is that, as the pulse drifts, loss processes have longer to act on the trailing edge of the injection pulse.

We also note that three important assumptions are made in order to apply the drift velocity calculation to the observations. First, we must assume that the field model is a reasonable approximation to the real field in which the particles are drifting. Since the field is less distorted after an injection and since the angle through which the particles drifted is small the results are not particularly sensitive to this assumption. Second we assume that the dominant motion is gradient and curvature drift. No **E**×**B** drifts were included in the calculations except for corotation drift. The good convergence of the projections for different energies in Figure 6 implies that, for these energies, over these short distances, this is a good approximation. Implicit in this assumption as well is that adiabatic motion conserving the first two invariants is maintained. Third, since we use spin-averaged fluxes, we must assume a representative pitch angle for the gradient-curvature drift calculations. *Reeves et al.,* [1991] have shown that α=45° produces consistent results in multispacecraft studies using spin-averaged data, and therefore we have used that value in this analysis. Finally, it is important to note that it is the amount of energy dispersion which determines the injection time. Therefore the calculated injection times are not subject to possible errors caused by the above assumptions. It is only the injection location which could be effected. Furthermore, the possible errors in the determination of the injection locations are estimated to be less than 5°.

Having found the location of origin of the electron peaks (which lie close to the eastern edge of the injections), we would then like to determine the location of the western edge of the injections to know their full local time extent. In earlier studies we have used the drift of the ions to determine the western boundary of the injection. However, for this event there is no spacecraft located near the western edge, and by the time the ions have drifted around the Earth to spacecraft 1977-007 the ion injection signature is too weak and noisy to resolve the necessary structure. To circumvent this problem, we may obtain a rough estimate of the local time extent of each injection event by considering the duration of each injection pulse as it drifts past the spacecraft. Figure 8 shows electron fluxes in the energy range 140-200 keV. In the higher-energy channels the three pulses can be resolved and their durations measured. By dividing the duration of the injection pulse by the drift velocity of the slowest

electrons in each energy band we can estimate the spatial extent of the injection region. The means and standard deviations from measurements at 95, 140, and 200 keV are 25° ± 2° for injection 1, 28° ± 0.5° for injection 2, and 110° ± 7° for injection 3. In fact, the standard deviations do not represent the full error in these estimates. More reasonable values would be ±5° for the first two injections and ±10° for the third injection. The standard deviations do, however, represent how consistently the apparent spatial extent of the injections can be determined. Finally we note that our calculation of the apparent spatial extent of the injection region assumes the injection takes place instantaneously rather than over a finite period of time. Other studies which do include ion measurements have shown that the duration of the injection pulse tends to overestimate the local time extent of the injection region [*Reeves et al.*, 1991].

INTERPRETATION OF THE EVENT

Geosynchronous observations of the CDAW 7 substorm add significant new information yet fit into a remarkably consistent scenario in which significant substorm processes take place in the ionosphere, in the outer radiation belts, and in the near-Earth tail.

Substorm Onset

Competing substorm theories place considerable emphasis on the location of substorm onset. We are fortunate in this event to have observations in the three key regions in which competing models place the initiation of the substorm. However, even in this case, the observations are subject to various interpretations. The first evidence of any activity in the midnight sector occurred at Cape Wellen, Siberia, when, at approximately 1107 UT, the *H* component of the magnetic field began a gradual, steady decrease. The *D* and *Z* components at Cape Wellen and all three components of the magnetic field recorded at College, Alaska, show distinct changes at approximately 1110 UT. By 1112 UT the strong *H* perturbation at College indicates that a substantial electrojet had developed. Which of these signatures indicates "onset" of the substorm? Clearly, as early as 1107 UT, there were local currents flowing in the Cape Wellen sector. However, the skeptical reader will also notice that there are distinct magnetic field variations observed at College as early as 1030 UT. We suggest that, just as a preexisting arc can brighten at onset, a preexisting current can intensify at onset. Therefore we propose that the best indication of onset in these data is the time at which large-scale ionospheric current activity commences and therefore suggest 1110 UT as our best estimate of onset (in general agreement with earlier studies).

At ISEE 2 the first signature of the substorm was observed, starting at approximately 1112 UT, as an increase in energetic particle fluxes [*Kettmann et al.,* 1990], an increase in plasma pressure, and tailward flows [*Hones et al.,* 1986]. This implies a delay of approximately 2 min after onset was observed on the ground. It does not, however, imply that reconnection in the tail followed onset on the ground unless ISEE 2 was located exactly at the *X* line whereas, in fact, ISEE 1 and 2 were located near the northern lobe. In an interpretation based on the traditional near-Earth neutral line model, reconnection onset would have begun at 1110 UT as evidenced by diversion of the cross-tail current into the ionosphere. The first signatures at ISEE would be observed when the field lines near ISEE began to reconnect. In a modification of the traditional neutral line model proposed by *Baker and McPherron* [1990] reconnection in the tail may begin in the growth phase (prior to 1110 UT) but that initially current is diverted to adjacent regions of the tail rather than along field lines into the ionosphere consequently enhancing the cross-tail currents earthward of the reconnection region. In this model there is no signature of the onset of reconnection on the ground. We also note the validity of the alternative hypothesis: that a current disruption region formed in the inner magnetosphere at 1110 UT prior to reconnection in the tail and we will discuss this scenario in more detail in a later section.

The important conclusion regarding substorm onset for this study is that both the ground magnetometers and the ISEE instruments observed substorm signatures several minutes prior to the onset of the first injection at geosynchronous orbit.

A Neutral Line Interpretation

In this section we assume that activity at the near-Earth neutral line is responsible for the injections and consider the implications. In the next section we will assume that current sheet disruptions are the cause of the injections and reinterpret the observations in that context.

The first injection of energetic particles on the drift shell sampled by spacecraft 1977-007 occurred at 1113:48 UT ±30 s. Magnetograms suggest that substorm onset occurred approximately 4 min earlier and ISEE measurements show signatures of plasmoid formation approximately two minutes before the injection. Thus, if reconnection in the tail is responsible for the geosynchronous injections, a time delay is clearly implied. *Russell and McPherron* [1973] discussed an earthward propagating compression wave which communicates between reconnection in the tail and substorm injections at geosynchronous orbit. In this case the delay between onset and injection is the propagation time of the wave. For the CDAW 7 substorm we can estimate the average velocity at which such a disturbance

would have to propagate earthward. To do so, we must first know the location of the reconnection region. *Kettmann et al.* [1990] looked for time-of-flight dispersion in the ions observed by ISEE-2. On a time scale of 12 s (the time delay between subsequent proton spectra) there was no energy dispersion seen in the arrival of the tailward flowing protons. This suggests a source region not more than 4.5 R_E earthward of ISEE-2. In other words, the reconnection region was most likely located between 16.5 and 21 R_E down the tail.

A lower bound on the communication speed between reconnection onset and the first injection is obtained by taking onset at 1110 UT and the reconnection location at 21 R_E. This implies an average convection speed of approximately 400 km/s. An upper bound is obtained by taking the time of the pressure pulse at ISEE (1112 UT) and the closer distance of 16.5 R_E which gives a speed of about 850 km/s. This is admittedly a crude estimate but it is less than or of the order of typical Alfvén velocities in the tail [e.g., *Lui,* 1987] and therefore provides a plausible explanation for the time delay. It must be noted though that, to be consistent with the common observation of dispersionless injections, any proposed mechanism of propagation must be shocklike in that it must not produce energy dispersion in the energetic particles as it propagates.

The next issue is how tail reconnection can produce a flux enhancement. Figure 9*a* shows a sketch of a field line which has been stretched far down the tail to the vicinity of the reconnection region and then snaps back bringing energized particles with it. This is the model proposed by *Baker et al.* [1979]. We note, however, that for a geosynchronous field line to be stretched to approximately 20 R_E down the tail requires not only strong currents near the Earth [e.g., *Kaufmann,* 1987] but also requires that the currents remain strong over a quite extended portion of the tail.

In Figure 9*b* the geosynchronous field line in the tail is stretched but not all the way to the reconnection region. In this case a mechanism other than energization in the reconnection region must be responsible for the substorm injection. One possibility is through adiabatic particle energization due to field reconfiguration [e.g., *Lyons and Williams*, 1980]. As the field lines become more dipolelike, the field strengths along that field line increase and the mirror points move toward the equator and heat the particles through betatron and Fermi acceleration which raises the flux in a given energy band [e.g., *Williams et al.,* 1990]. The question then is whether this effect can produce enough heating to reproduce the observed changes in flux. This is a particular concern for the estimated 10-20% of substorms for which ions with energies > 300 keV are injected at expansion phase onset [*Baker,* 1984; *Belian et al.,* 1978]. We note that it is possible to produce higher energies if nonadiabatic motion is invoked (for example, if convection occurs on a time scale

which is fast compared to the bounce time) but that at present no quantitative theory exists for how the neutral line produces injections at geosynchronous orbit.

The final question is how (even qualitatively) the reconnection process produces the multiple injections that were observed during this event. Figure 10 shows a time line for the CDAW-7 substorm based on ISEE and geosynchronous spacecraft data. It is apparent that the total energy dissipated in the CDAW-7 substorm is not released at once nor is it dissipated continuously. Three injections occur and, comparing the time line of *Kettmann et al.* [1990], two of those occur after the last closed field line reconnected (1115:20 UT) and the plasmoid exited down the tail leaving ISEE-2 in the lobes (1117 UT). The second injection occurred only about 4 min after the first injection and about 6 min after onset. This is shorter than typical growth phase time scales [*McPherron,* 1970; *Baker et al.,* 1978]. Furthermore, ISEE 1 and 2 did not observe plasma sheet recovery. Therefore we believe that the first two injections are part of the same substorm. Both the size and the duration of the flux increase for the first and the second injection (Figure 7) are comparable suggesting they release comparable amounts of stress in the magnetotail. They also span similar local time extents.

The third injection took place at 1134:48, nearly 17 min after the second injection (Figure 10). As discussed earlier, this injection appears to be the largest and the terminal event of the substorm. It spans up to 4 times as large a range of local times as the previous two injections. It corresponds closely with the peaks in the *AE* and *AL* indices (Figure 3) and is followed some 6 min later by recovery of the plasma sheet at ISEE locations. Although the 17 min between the second and third injections is still shorter than typical growth phase time scales (30-120 min), the data allow the possibility that the third injection is actually a separate "substorm" with the usual connotations of that term [*Akasofu*, 1964]. However, it is clear from the magnetograms, from *AE* and *AL*, and from ISEE that if a recovery occurred between the second and third injections it was incomplete. Furthermore, since the third injection is the largest, the negative *H* bay after 1135 UT is deepest, and *AE* and *AL* are at their peaks it appears that the 1118 UT injection did not dissipate all of the previously stored energy. These observations and the close association of recovery at ISEE within 6 min of the third injection lead us to conclude that, like the second injection, it was part of the same substorm.

How then are these later injections produced? The second injection occurs approximately 160 s after the reconnection of the last closed field line so it may be that the exit of the plasmoid somehow produces an enhancement in the relaxation of the field. But this would not explain the third injection. Considering Figure 9*b*, we can hypothesize that the field dipolarized and energized particles in three distinct steps, but this proposition is

more difficult than accounting for a single injection by this mechanism. Figure 2 and data from other electron channels (not shown) indicate that not only were electrons with energies >300 keV injected during the CDAW 7 substorm but that each of the three injections contained > 300-keV electrons. Therefore, if betatron and Fermi acceleration energizes the plasma, it must do so in three steps each of which produces > 300-keV electrons. Furthermore, since the plasma energized in this way is carried with the field lines, and since the injections overlap in local time, the three-step dipolarization must take place in the same location in space, namely at geosynchronous orbit near midnight. We can also postulate that the later injections could be due to an enhanced rate of reconnection of open field lines and that particles are directly energized there (Figure 9*a*). Two difficulties arise here. We know of no mechanism proposed which would produce impulsive bursts of reconnection of open field lines, and lobe field lines have relatively few particles to accelerate yet the third injection was the largest.

Since neither of the above processes yields ready interpretation of the cause of the second and third injections, we conclude that if the injections are produced by activity at the *X* line that it is most likely that multiple *X* lines form on closed field lines. The first possibility is that the *X* line moves in the GSE *Y* direction and reconnects field lines at a different local time. In this case, reconnection regions do not overlap in local time but the injection regions do. Therefore the transport cannot be purely radial and must vary from one injection to another.

It is also possible that the reconnection region moves in radius. This scenario seems the most plausible of those which assume that the reconnection region is the source of the injections. It is illustrated in Figure 11. In Figure 11*a* the magnetosphere is in a loaded configuration prior to the substorm. The ISEE spacecraft are near the lobes but within the plasma sheet. In Figure 11*b* the first episode of reconnection begins. ISEE 2 measures an ion pressure pulse and tailward streaming energetic ions in the separatrix layer which moves north across ISEE 2. The first injection occurs and by 1117 the exit of the plasmoid has left the ISEE spacecraft in the lobes. In Figure 11*c* a second period of rapid reconnection in the near-Earth plasma sheet produces a second plasmoid. As more energy is released, the magnetic field relaxes again and a second injection peak is observed at geosynchronous orbit. Although this is a two-dimensional picture, it must be a three-dimensional process with the new reconnection region spanning a new range of local times. Other evidence for multiple plasmoids was presented by *Slavin et al.* [1984] who studied traveling compression regions (TCRs), which are interpreted as the lobe signatures of the ejection of plasmoids. In one of three events illustrated, two TCRs were separated by only 15 min which was also interpreted as evidence for multiple plasmoid ejections.

We conclude from this rather lengthy discussion that it is possible to account for all the observations (ISEE, magnetometer, and geosynchronous) within the context of the near-Earth neutral line model but that accounting for the two injections which occurred after the exit of the plasmoid requires significant modifications of that model such as azimuthal motion of the neutral line within the tail, bursts of reconnection on open field lines, or possible formation of multiple plasmoids. In addition, there is still little understanding of exactly how reconnection in the tail produces geosynchronous injections.

A Current Sheet Disruption Interpretation

An interpretation of the multiple injections observed by spacecraft 1977-007 during the CDAW 7 substorm based on the current sheet disruption model is inherently simpler than an interpretation based on the neutral line model because a direct, local mechanism is responsible for the injections. Each injection is produced through energization of particles in turbulent magnetic fields associated with the disruption of the cross-tail current and its diversion into the ionosphere [e.g., *Lopez et al.,* 1989, 1990]. This idea is supported by the close association in time of the injections and ground magnetometer signatures (Figures 1-3). Note that each injection time was accompanied at College by the same signature – negative turnings of all three field components. However, we again find that there are three critical questions: (1) why was there a delay between onset and the first injection? (2) why is there a difference in the local time regions? and (3) how was a plasmoid (or the signatures expected of a plasmoid) produced near ISEE distances?

A schematic of the evolution of the current sheet disruption region has been presented by *Lopez et al.* [1990], and a similar schematic is shown in Figure 12. *Lopez et al.* [1990] propose that the line of constant β is an inner limit of current stability which is similar in shape to *McIlwain's* [1974] injection boundary. In this picture substorm onset (at 1110 UT) would be produced by a disruption of cross-tail current and diversion of that current into the ionosphere where it would produce the observed magnetic field changes. This current disruption would also produce a substorm injection at that time. Spacecraft 1977-007 did not observe an injection until almost 4 min later. However, *Lopez et al.* [1990] also propose that the disruption region (and hence the injection region) is initially quite localized and expands radially outward (Figure 12*a*). Therefore, according to that proposition it is possible that the initial current disruption occurred on a drift shell radially inward from the geosynchronous drift shell and therefore was not observed by 1977-007.

Subsequent injections are produced as the disruption region expands. (We note that the disruption region must expand impulsively, not continuously.) Consideration of the second

and third injections, though, requires that we modify Figure 12 somewhat. The partial recovery of the field at College before the 1135 UT injection implies that the cross-tail current may become reestablished between expansions. More importantly, the current disruption region does not necessarily expand. The first and second injections span approximately equal regions of local time at geosynchronous orbit (but could have different radial extents) and the injection region moves west. In this case the western edge appears to expand while the eastern edge appears to contract. Therefore we propose that current sheet disruption may be "patchy" as sketched in Figure 13. Each disruption occurs in a different (but possibly overlapping) local time sector and between disruptions the currents may at least partially reestablish themselves. It is important to note, with regard to Figures 12 and 13, that the analysis of the injections presented here tells us nothing of the radial extent of the injection region. Our data do not even exclude the possibility that an initial disruption at 1110 UT occurs on drift shell that is radially outward from geosynchronous rather than inward.

Thus we find that the current sheet disruption model can answer our first two questions with relatively slight modifications. The third question, how current disruption can produce plasmoid signatures at ISEE, is considerably more difficult. If we propose that somehow a current disruption starting at 1110 UT, which may even start earthward of geosynchronous orbit later results in reconnection in the tail then we run into at least two more problems. We must come up with a mechanism in which dipolarization of the field in the inner magnetosphere results in further thinning of the plasma sheet and reconnection in the tail. We must also consider the time sequence: 1110 UT, current sheet disruption occurs but is not observed at geosynchronous; 1112 UT, evidence of plasmoid formation at 21 R_E down tail; 1114 UT, current sheet disruption and substorm injection at geosynchronous. Rather than hypothesize and criticize such mechanisms in the next section we present a more straightforward interpretation.

A Simple Interpretation

Drawing on a series of recent ideas [*Lopez et al.,* 1990; *Baker and McPherron,* 1990; *Lui et al.,* 1990], we propose that elements of both the near-Earth neutral line model and the current sheet disruption model can be combined to produce a relatively simple picture of the CDAW 7 substorm which accounts for all the published observations. We propose that a plasmoid is produced by reconnection in the tail but that the injections are produced by current sheet disruption in the vicinity of geosynchronous orbit. In this interpretation reconnection in the tail is responsible for the first diversion of current into the ionosphere at

approximately 1110 UT. Reconnection may have begun at 1110 UT or somewhat before that time provided no current was diverted into the ionosphere until then [*Baker and McPherron,* 1990]. In this case there would be no current sheet disruption in the inner magnetosphere at 1110 UT, since the magnetometer signatures would be due to field-aligned currents produced near the *X* line region. Reconnection could not have started much before 1110 UT because ISEE observed a pressure pulse and tailward streaming at 1112 UT and was in the lobes by 1117 UT.

The field perturbations at 1110 UT are relatively small which would be expected if most of the current which is diverted around the *X* line region; above, below, earthward, and tailward. This enhances the current flowing in the region earthward of the neutral line which is exactly the condition which makes it more likely that instabilities will develop in the inner magnetosphere causing current sheet disruption there [*Lui et al.,* 1990]. The disruptions in the inner magnetosphere produce the injections observed by spacecraft 1977-007. The ejection of the plasmoid down the tail does not decrease the current flowing in the inner magnetosphere and therefore does not decrease the need for further current disruptions to bring the inner magnetosphere closer to its ground state. In fact the exit of the plasmoid downtail may increase the current density earthward of the *X* line by decreasing the size of the tail. The inner magnetosphere then relaxes toward its ground state through a series of three current disruptions [*Lopez et al.,* 1990] which divert current into the ionosphere, dipolarize the field, and energize particles producing the injections as described in the preceding section.

In this scenario, current sheet disruption does not produce the neutral line in the tail. Neither does the neutral line directly produce geosynchronous injections. Rather, the formation of a neutral line initially enhances the conditions which make current sheet disruptions (and therefore injections) more likely. An important implication is that, in other substorms, it is possible for the currents in the inner magnetosphere to build up to a point where a current sheet disruption occurs independent of and prior to the formation of a neutral line. The converse is not true. We would always expect inner magnetospheric current disruptions when a neutral line forms since they are the mechanism through which the field dipolarizes and approaches its ground state.

CONCLUSIONS

We have analyzed geosynchronous energetic particle data for the CDAW 7 substorm and compared the results with ISEE data and ground-based measurements. Three distinct peaks in the geosynchronous energetic particle flux were observed superimposed on a broad injection flux increase. In order to make a comparison with other observations it was

necessary to project the observations from spacecraft 1977-007 back to their origin on the geosynchronous drift shell. To do so, we calculated the bounce average drift velocity in the field model of *Tsyganenko and Usmanov* [1982]. The injection times and locations were determined from the convergence of the projection of observations at different energies back along the drift shell [*Reeves et al.,* 1990; 1991]. The first injection peak projected to 10° east of midnight. The second peak projected to -1° and the third peak to 0°. The three injections occurred at 1113:48, 1118:00, and 1134:48 (all ±30 s). From the duration of the energetic flux increases the maximum local time extents of the three injections were estimated to be 25°±5°, 28°±5°, and 110°±10° respectively.

We have combined these results with the ground magnetometer data and the results of earlier CDAW 7 studies of ISEE data and considered interpretations based on the near-Earth neutral line and current sheet disruption substorm models. We have reexamined the magnetometer data for this event by using all three components of the magnetic field measured at College, Alaska, and Cape Wellen, Siberia. On the basis of this data we propose 1110 UT ± 1 min as a best determination of substorm onset which is somewhat earlier than previous studies. We find that either the neutral line or the current disruption model can account for this onset time in relationship to subsequent substorm processes.

Assuming that the first injection is associated with onset of reconnection in the near-Earth plasma sheet we have calculated the velocity at which information must be conveyed from the tail to geosynchronous orbit. On the basis of the delay time between onset and the first injection and the estimated distance from the geosynchronous drift shell to the reconnection region we were able to estimate the velocity of propagation to be 400-850 km/s. This estimate is admittedly rather crude but to our knowledge it is the first such estimate to appear in the literature.

We considered various mechanisms by which reconnection in the magnetotail could be responsible for the three injections at geosynchronous orbit. A key observation is that the second and third injections occurred after the ejection of the plasmoid down the tail and before the recovery of the plasma sheet at ISEE. We found that a satisfactory explanation of the observations could be obtained by considering significant extensions to the standard near-Earth neutral line model such as episodic bursts of reconnection of open field lines or the formation of multiple plasmoids by the creation of new reconnection regions. An important constraint on multiple *X* line models is provided by the overlap in local time of the three regions from which the individual injections originated.

The current sheet disruption model does a good job at explaining the ground magnetometer and the geosynchronous observations. The onset at 1110 UT which was not accompanied by an injection at geosynchronous orbit can be explained by the existence of a

disruption region and injection which were localized on drift shells not sampled by the 1977-007 spacecraft. The variation in the local time extent of the three calculated injection regions can be explained by modifying the picture of *Lopez et al.* [1990] to allow for "patchy disruptions" which may move their position without necessarily expanding in local time. However, the current disruption model makes no predictions as to the ISEE observations in the tail.

Each model appears to work well in the region in which its main processes occur but each model had a hard time explaining the observations in the other region. Therefore we propose a simple model which combines the best elements of both models and explains all the major CDAW 7 observations without invoking additional, unobserved plasmoids or current disruptions and injections. We suggest that reconnection in the tail produced the magnetic field perturbations observed on the ground at 1110 UT and the pressure pulse, tailward streaming, and energetic particle signatures observed at ISEE starting at 1112 UT. Some of the cross-tail current was diverted into the ionosphere while much of it was diverted earthward but continued in the cross-tail direction [*Baker and McPherron,* 1990]. This added current creates an unstable condition [*Lui et al.,* 1990] which results in current disruption, dipolarization of the field, and energetic particle injection. The field relaxes toward its ground state in this manner in three distinct steps which produce the three observed injections.

One unambiguous conclusion of this study is that the CDAW 7 substorm was considerably more complex than indicated by the ISEE data alone. The ability to project geosynchronous energetic particle observations back from their point of observation to their point of origin removes the constraint that a spacecraft be located within the injection region itself and enhances the opportunity for multispacecraft studies of substorms.

Acknowledgments. This work was done under the auspices of the U.S. Department of Energy and was supported in part by the Geosciences Program of the DoE Office of Basic Energy Science.

The Editor thanks W. Lennartsson and R. Lopez for their assistance in evaluating this paper.

REFERENCES

Akasofu, S.-I., The development of the auroral substorm, *Planet. Space Sci., 12*, 273, 1964.

Andrews, M. K., E. Keppler, and P. W. Daly, Plasma sheet motions inferred from medium energy ion measurements, *J. Geophys. Res., 86,* 7543, 1981.

Baker, D. N., Particle and field signatures of substorms in the near magnetotail, in Magnetic Reconnection in Space and Laboratory Plasmas, *Geophys. Monogr. Ser.*, Vol 30, edited by E. W. Hones, Jr., p.193, AGU, Washington D. C., 1984.

Baker, D. N., P. R. Higbie, E. W. Hones, Jr., and R. D. Belian, High-resolution energetic particle measurements at 6.6 R_E, 3, Low-energy electron anisotropies and short-term substorm predictions, *J. Geophys. Res., 83*, 4864, 1978.

Baker, D. N., R. D. Belian, P. R. Higbie, and E. W. Hones, High-energy magnetospheric protons and their dependence on geomagnetic and interplanetary conditions, *J. Geophys. Res., 84*, 7138, 1979.

Baker, D. N., E. W. Hones, Jr., D. T. Young, and J. Birn, The possible role of ionospheric oxygen in the initiation and development of plasma sheet instabilities, *Geophys. Res. Lett., 9*, 1337, 1982.

Baker, D. N., and R. L. McPherron, Extreme energetic particle decreases near geostationary orbit: A manifestation of current diversion within the inner plasma sheet, *J. Geophys. Res., 95*, 6591, 1990.

Baumjohann, W., G. Paschmann, and C. A. Catell, Average plasma properties in the central plasma sheet, *J. Geophys. Res., 94,* 6597, 1989.

Baumjohann, W., G. Paschmann, and H. Lühr, Characteristics of high-speed flows in the plasma sheet, *J. Geophys. Res., 95,* 3801, 1990.

Belian, R. D., D. N. Baker, P. R. Higbie, and E. W. Hones, Jr., High-resolution energetic particle measurements at 6.6 R_E, 2; High-energy proton drift echoes, *J. Geophys. Res., 83*, 4857, 1978.

Belian, R. D., D. N. Baker, E. W. Hones, and P. R. Higbie, High-energy proton drift echoes: Multiple peak structure, *J. Geophys. Res., 84,* 9101, 1984.

Daly, P. W., and E. Keppler, Remote sensing of a flux transfer event with energetic particles, *J. Geophys. Res., 88,* 3971, 1983.

Eastman, T. E., G. Rostoker, L. A. Frank, C. Y. Huang, and D. G. Mitchell, Boundary layer dynamics in the description of magnetospheric substorms, *J. Geophys. Res., 93,* 14,411, 1988.

Fritz, T. A., D. N. Baker, R. L. McPherron, and W. Lennartsson, Implications of the 1100 UT March 22, 1979, CDAW 6 substorm event for the role of magnetic reconnection in

the geomagnetic tail, in Magnetic Reconnection in Space and Laboratory Plasmas, *Geophys. Monogr. Ser.*, Vol 30, edited by E. W. Hones, Jr., p.203, AGU, Washington D. C., 1984.

Higbie, P. R., R. D. Belian, and D. N. Baker, High-resolution energetic particle measurements at 6.6 R_E 1: Electron micropulsations, *J. Geophys. Res., 83*, 4857, 1978.

Hones, Jr., E. W., Transient phenomena in the magnetotail and their relation to substorms, *Space Sci. Rev., 23,* 393, 1979.

Hones, Jr., E. W., T. A. Fritz, J. Birn, J. Cooney, and S. J. Bame, Detailed observations of the plasma sheet during a substorm on April 24, 1979, *J. Geophys. Res., 91*, 6845, 1986.

Kaufmann, R. L., Substorm currents: Growth phase and onset, *J. Geophys. Res., 92*, 7471, 1987.

Kettmann, G., T. A. Fritz, and E. W. Hones Jr., CDAW 7 revisited: Further evidence for the creation of a near-Earth substorm neutral line, *J. Geophys. Res., 95,* 12,045, 1990.

Lopez, R. E., and A. T. Y. Lui, A multisatellite case study of the expansion of a substorm current wedge in the near-Earth magnetotail., *J. Geophys. Res., 95*, 8009, 1990.

Lopez, R. E., D. N. Baker, A. T. Y. Lui, D. G. Sibeck, R. D. Belian, R. W. McEntire, T. A. Potemra, and S. M. Krimigis, The radial and longitudinal propagation characteristics of substorm injections, *Adv. Space. Res., 8*, 91-95, 1988.

Lopez, R. E., D. G. Sibeck, R. W. McEntire, and S. M. Krimigis, The energetic ion substorm injection boundary, *J. Geophys. Res., 95*, 109, 1990.

Lui, A. T. Y., Magnetotail Physics, p. 8, Johns Hopkins University Press, Baltimore, MD., 1987.

Lui, A. T. Y., R. E. Lopez, S. M. Krimigis, R. W. McEntire, L. J. Zanetti, and T. A. Potemra, A case study of magnetotail current sheet disruption and diversion, *Geophys. Res. Lett, 15*, 721, 1988.

Lui, A. T. Y, A. Mankofsky, C.-L. Chang, K. Papadopoulos, and C. S. Wu, A current disruption mechanism in the neutral sheet for triggering substorm expansions, *Geophys. Res. Lett., 6,* 745, 1990.

Lyons, L. R., and D. J. Williams, A source for the geomagnetic storm main phase ring current, *J. Geophys. Res., 85*, 523, 1980.

McIlwain, C. E., Substorm injection boundaries, in Magnetospheric Physics, edited by B. M. McCormac, p. 143, D. Reidel, Hingham, Mass, 1974.

McPherron, R. L., Growth phase of magnetospheric substorms, *J. Geophys. Res., 75,* 5592, 1970.

McPherron, R. L., C. T. Russell, and M. P. Aubry, Satellite studies of magnetospheric substorms on August 15, 1968, 9, Phenomenological model for substorms, *J. Geophys. Res., 78,* 3131, 1973.

Nagai, T., D. N. Baker, and P. R. Higbie, Development of substorm activity in multiple-onset substorms at synchronous orbit, *J. Geophys. Res., 88*, 6994, 1983.

Reeves, G. D., R. D. Belian and T. A. Fritz, Numerical tracing of energetic particle drifts in a model magnetosphere, *J. Geophys. Res., 96,* 13,997, 1991.

Reeves, G. D., T. A. Fritz, T. E. Cayton, and R. D. Belian, Multi-satellite measurements of the substorm injection region, *Geophys. Res. Lett., 17,* 2015, 1990.

Roederer, J. G., Dynamics of Geomagnetically Trapped Radiation, Springer-Verlag, New York, 1970.

Russell, C. T., The ISEE 1 and 2 fluxgate magnetometers, *IEEE Trans. Geosci. Electron., GE-16*, 239, 1978.

Russell, C. T., and R. L. McPherron, The magnetotail and substorms, *Space Sci. Rev., 15*, 205, 1973.

Slavin, J. A., E. J. Smith, B. T. Tsuratani, D. G. Sibeck, H. J. Singer, D. N. Baker, J. T. Gosling, E. W. Hones, and F. L. Scarf, Substorm associated traveling compression regions in the distant tail: ISEE 3 geotail observations, *Geophys. Res. Lett., 7*, 657, 1984.

Takahashi, K, L. J. Zanetti, R. E. Lopez, R. W. McEntire, T. A. Potemra, and K. Yumoto, Disruption of the magnetotail current sheet observed by AMPTE CCE, *Geophys. Res. Lett., 14,* 1019, 1987.

Tsyganenko, N. A., and A. V. Usmanov, Determination of the magnetospheric current system parameters and development of experimental geomagnetic field models based on data from IMP and HEOS satellites, *Planet. Space Sci., 30*, 985, 1982.

Wiens, R. G., and G. Rostoker, Characteristics of the development of the westward electrojet during the expansion phase of magnetospheric substorms, *J. Geophys. Res., 80*, 2109, 1975.

Williams, D. J., E. Keppler, T. A. Fritz, B. Wilken, and G. Wibbernez, The ISEE 1 and 2 medium energy particles experiment, *IEEE Trans. Geosci. Electron., GE-16*, 270, 1978.

Williams, D. J., D. G. Mitchell, C. Y. Huang, L. A. Frank, and C. T. Russell, Particle acceleration during substorm growth phase, *Geophys. Res. Lett.*, 17, 587, 1990.

Yahnin, A. G., T. Bosinger, J. Kangas, and R. D. Belian, Some implications of multiple peak structure of drifting high energy proton clouds for substorm dynamics as inferred from ground satellite correlations, *Ann.s Geophys., 8*, 327, 1990.

R. D. Belian, T. A. Fritz, G. Kettmann, and G. D. Reeves, Los Alamos National Laboratory, Los Alamos, NM 87545.

(Received June 10, 1991;
revised October 18, 1991;
accepted December 11, 1991.)

Paper number 91JA03103.
0148-0227/92/91JA-03103 $05.00

FIGURE CAPTIONS

Fig. 1: The magnetogram from College, Alaska. Substorm onset begins with the negative bay at approximately 1110 UT which is marked with a dotted line. Three other times are marked with solid lines. These are the approximate times of geosynchronous particle injections. Strong perturbations in the magnetic field components are closely associated with these times.

Fig. 2: The magnetogram from Cape Wellen, Siberia. The times are marked as in Figure 1. Of note are the gradual decrease in the *Z* component without sharp perturbations and the downward turning of the *H* component beginning at approximately 1107 UT.

Fig. 3: The *AE* and *AL* auroral indices for the period 1100 to 1200 UT. The times are marked as in Figure 1.

Fig. 4: The CDAW 7 substorm injection as seen in differential electron flux from the CPA instrument on spacecraft 1977-007 as a function of time. Flux profiles have been off-set on the scale so that the injection features can be seen more clearly. Three injection peaks can be seen superimposed on the overall flux increase. All three show dispersion.

Fig. 5: The 65-950 keV differential electron flux from the CPA instrument as a function of time. Three injection peaks can be identified superimposed on a broad injection profile (shaded).

Fig. 6: Projections along the drift shell for the second electron injection peak observed at 1977-007. The observation point for each energy is in the upper right corner. Lines for all energies converge very closely at 1118:00 and -1° from local midnight. This point defines the time and location at which electrons associated with this feature were injected onto the geosynchronous drift shell.

Fig. 7: A schematic of the times and locations of geosynchronous injection features. Local midnight is defined as 0° and positive values are to the east. The "electron edge" is defined by the first electrons seen at the spacecraft and

defines the easternmost extent of the injection region. The projected injection location for the three peaks are indicated by black dots. The electron peaks originate at points close to the eastern edge of the injection region and range from 10° to -1°. Injection times range from 1113:48 to 1134:48. The range of local times spanned by the injection region (shaded bars) is estimated from the duration of the injection peaks. For the first two injections the ranges are 25°±5° and 28°±5°. For the third peak the range is estimated to be 110°±10° and extends off the scale.

Fig. 8: The differential electron count rate from the CPA instrument in the range 140-200 keV. The duration of each of the three peaks is shown. From the duration and the model drift velocity the spatial extent of each injection can be estimated. For the slowest particles in the three highest electron energies channels (95, 140, and 200 keV) the estimated spatial extents agree very closely. For lower energies the first two peaks begin to overlap.

Fig. 9: A schematic of possible injection mechanisms. (*a*) The geosynchronous field line is initially highly distorted and is stretched to the reconnection region. Charged particles are energized directly and convected back to the geosynchronous region as the field collapses. (*b*) The geosynchronous field line is stretched but not to the reconnection region. Betatron, Fermi, or nonadiabatic acceleration processes may produce the observed injection.

Fig. 10: A time line for events observed at (top) ISEE and at (bottom) geosynchronous orbit. Times are rounded to the nearest minute although some are known more accurately (see text).

Fig. 11: This figure shows, in the noon-midnight plane, a possible interpretation of the ISEE and geosynchronous data based on an extension of the near-Earth neutral line model. Spacecraft are shown at the approximate locations of ISEE and 1977-007. The shaded volume represents the relatively dense plasma sheet. (*a*) The magnetotail lobes are loaded with flux and the plasma sheet thins. (*b*) The first episode of reconnection takes place within 4.5 R_E earthward of ISEE 2. (*c*) A second plasmoid is formed by pinching off closed field lines at a new reconnection region which is probably earthward of the first reconnection region.

Fig. 12: A schematic of the current sheet disruption mechanism based on Figure 11 of *Lopez et al.* [1990]. (*a*) Onset is defined by a current sheet disruption which occurs within a localized region of the inner magnetospheric current sheet and bounded earthward by a surface which represents the limits of current stability (Ω=0). Within the disruption region (shaded) magnetic fields are turbulent and plasma is energized to produce a substorm injection. At the edges of the disruption region, current is diverted into the ionosphere. (*b*) The region of current disruption expands radially and azimuthally but is still bounded by the Ω=0 surface. (*c*) The current disruption region continues to expand until the geomagnetic field approaches its ground state.

Fig. 13: A modification of Figure 12 which is more consistent with the CDAW 7 geosynchronous observations. (*a*) Current disrupts in a localized region as in Figure 11*a*. (*b*) A second current disruption occurs in a new localized area. The second injection occurs in an area independent of (but partially overlapping) the region of the first disruption and is not an expansion along a boundary. (*c*) The final injection covers all or most of the evening sector. The radial extent of the disruption-injection regions is completely arbitrary.

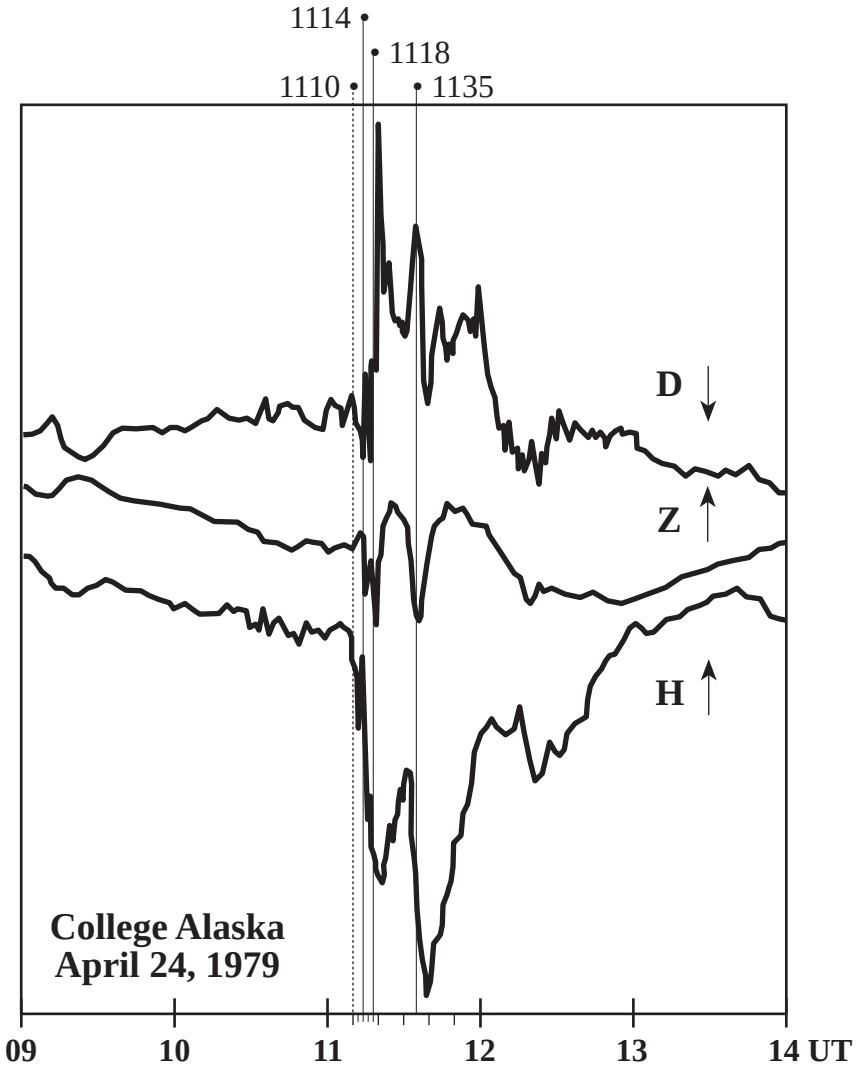
1114
1118
1110
1135
D
Z
H
College Alaska
April 24, 1979
09
10
11
12
13
14 UT

Fig. 1

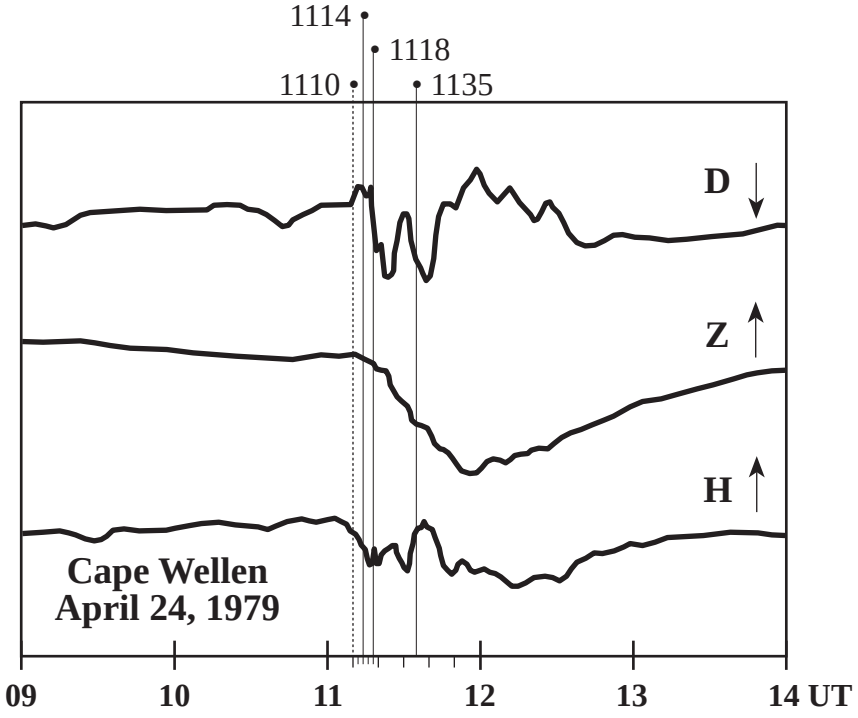
1114
1118
1110
1135
D
Z
H
Cape Wellen
April 24, 1979
09
10
11
12
13
14 UT

Fig. 2

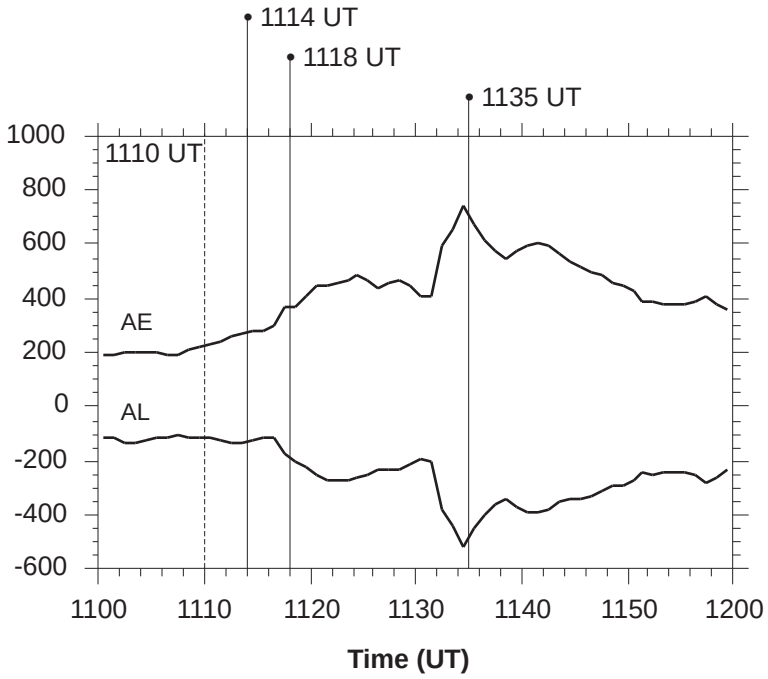
1114 UT
1118 UT
1135 UT
1110 UT
1000
800
600
400
200
0
-200
-400
-600
AE
AL
1100
1110
1120
1130
1140
1150
1200
Time (UT)

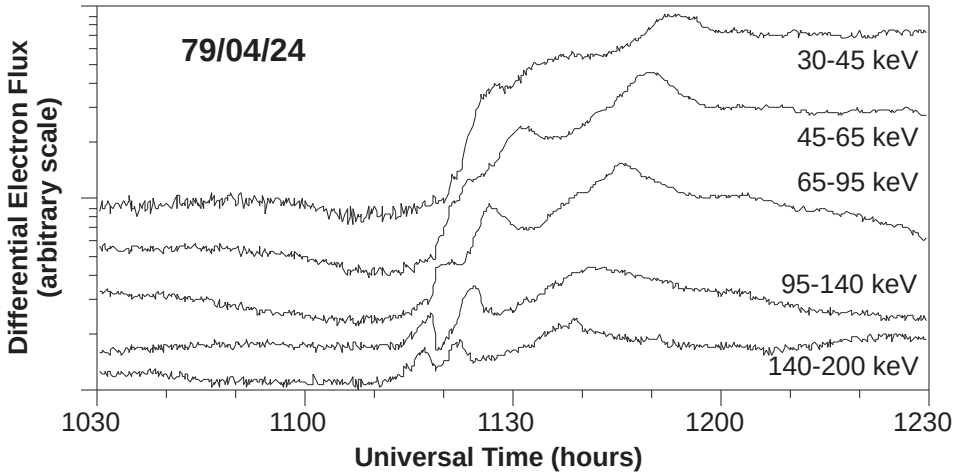
79/04/24
30-45 keV
45-65 keV
65-95 keV
95-140 keV
140-200 keV
Differential Electron Flux
(arbitrary scale)
1030
1100
1130
1200
1230
Universal Time (hours)

Figure 4

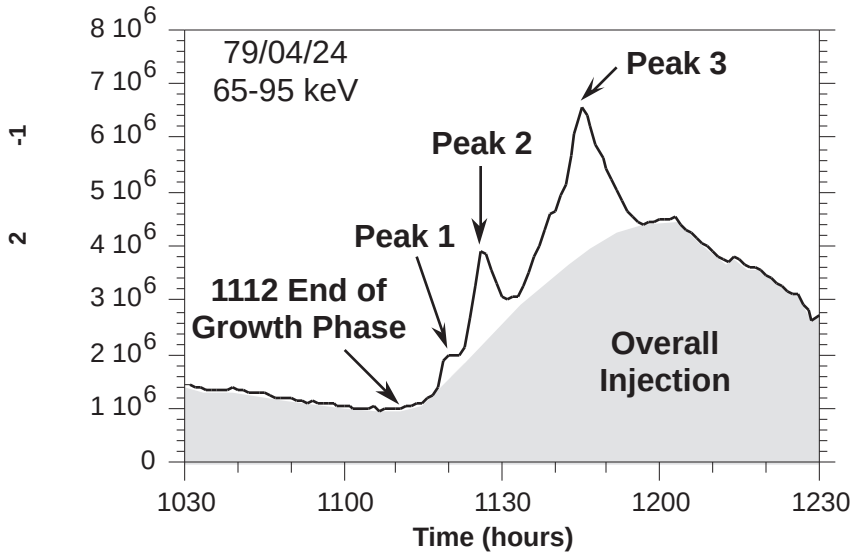
79/04/24
65-95 keV
Peak 3
Peak 2
Peak 1
1112 End of
Growth Phase
Overall
Injection
8 10^6
7 10^6
6 10^6
5 10^6
4 10^6
3 10^6
2 10^6
1 10^6
0
1030
1100
1130
1200
1230
Time (hours)
2 -1

Figure 5

Figure 6

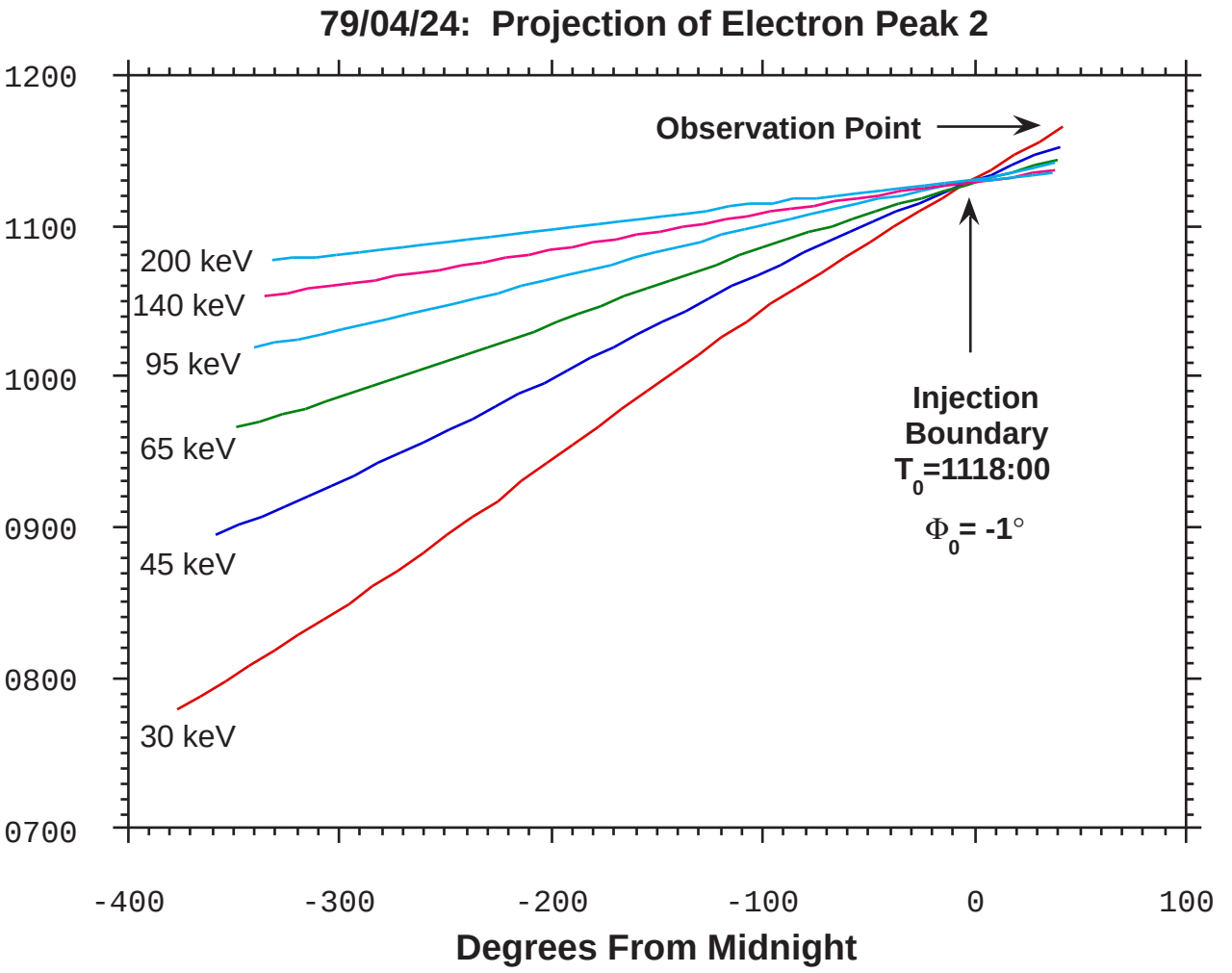
79/04/24: Projection of Electron Peak 2
1200
1100
1000
0900
0800
0700
-400
-300
-200
-100
0
100
Degrees From Midnight
Observation Point
200 keV
140 keV
95 keV
65 keV
45 keV
30 keV
Injection
Boundary
T0=1118:00
Φ0= -1°

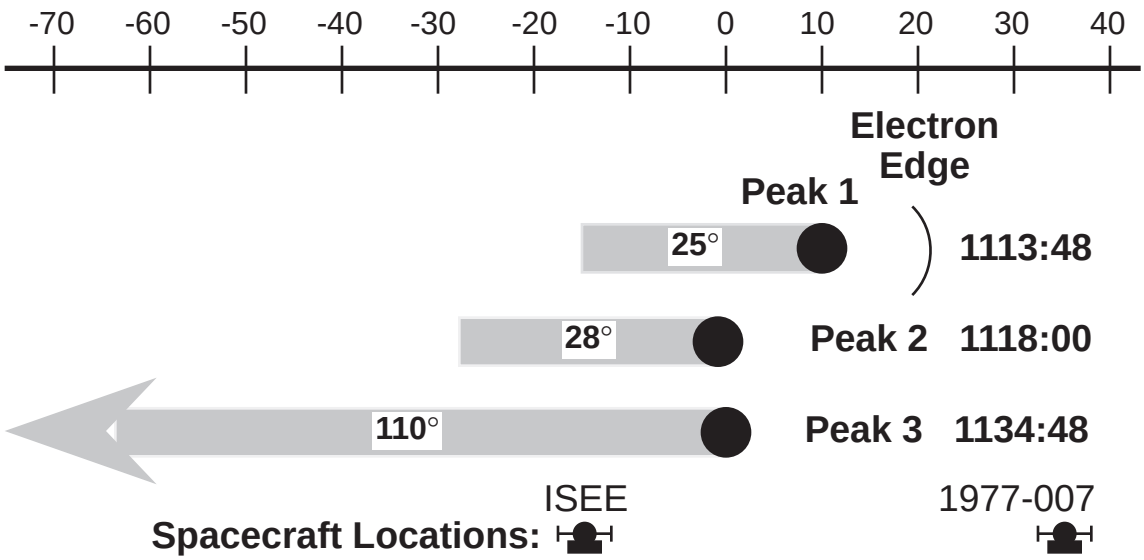
-70
-60
-50
-40
-30
-20
-10
0
10
20
30
40
Electron Edge
Peak 1
25°
1113:48
28°
Peak 2
1118:00
110°
Peak 3
1134:48
ISEE
1977-007
Spacecraft Locations:

Figure 7

Figure 8

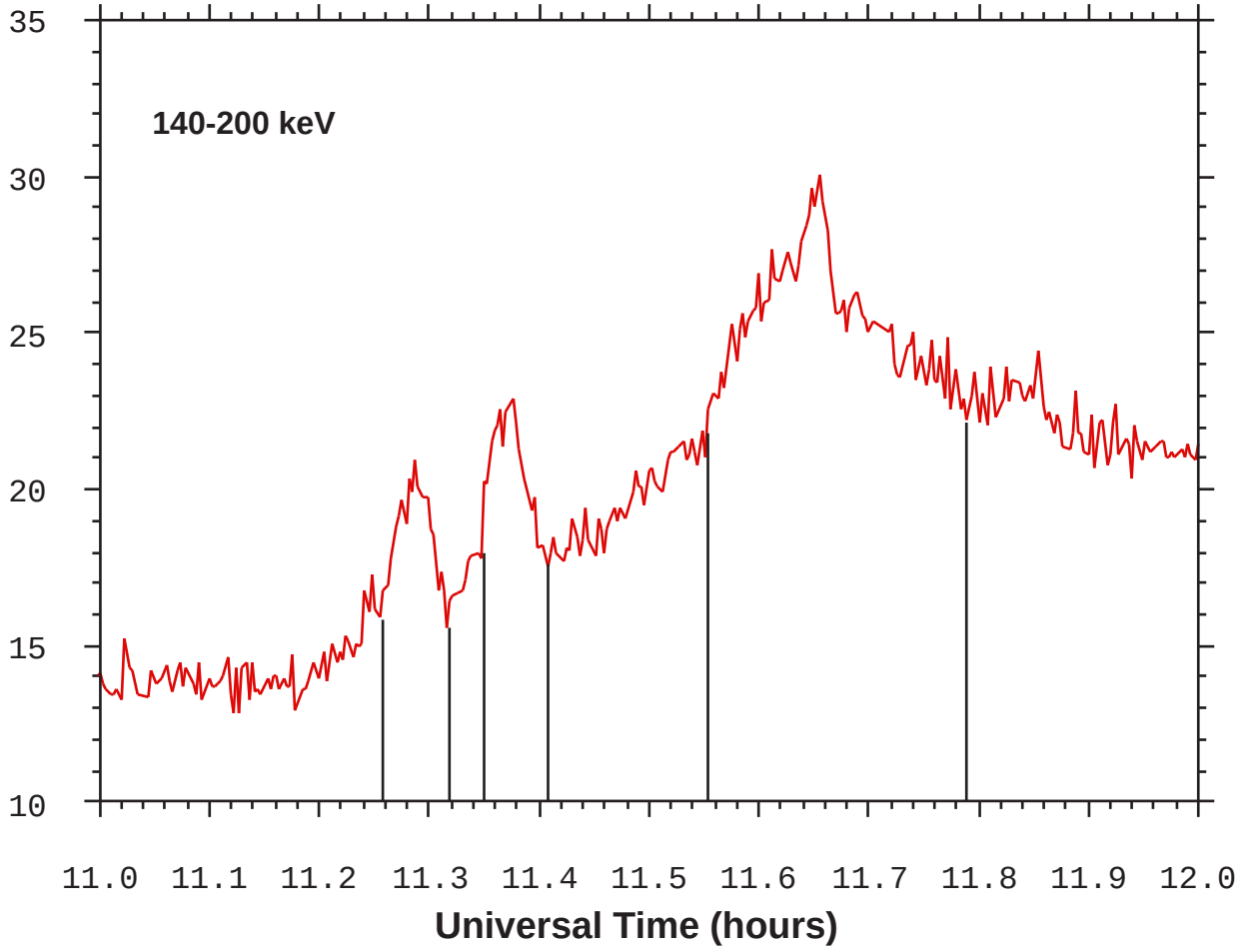
140-200 keV
35
30
25
20
15
10
11.0
11.1
11.2
11.3
11.4
11.5
11.6
11.7
11.8
11.9
12.0
Universal Time (hours)

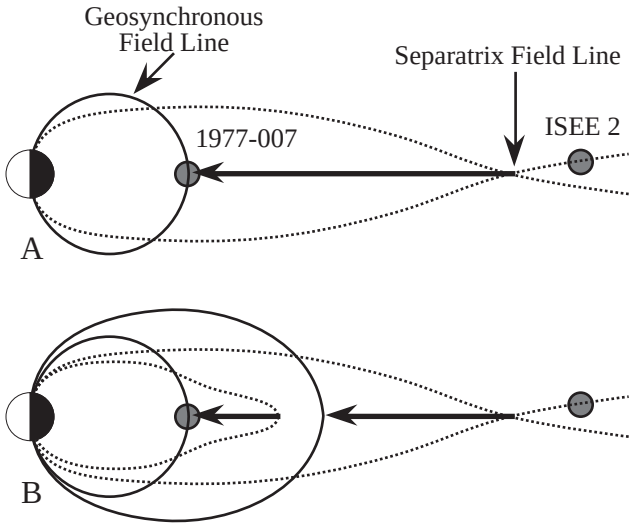
Geosynchronous
Field Line
Separatrix Field Line
ISEE 2
1977-007
A
B

Figure 9

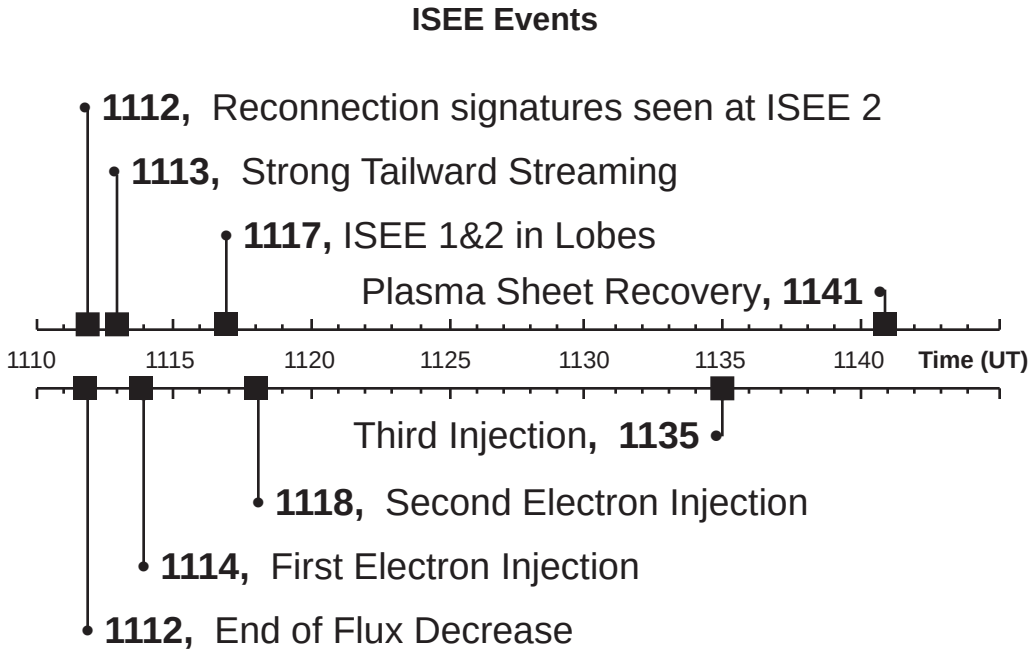
ISEE Events
1112, Reconnection signatures seen at ISEE 2
1113, Strong Tailward Streaming
1117, ISEE 1&2 in Lobes
Plasma Sheet Recovery, 1141
1110
1115
1120
1125
1130
1135
1140
Time (UT)
Third Injection, 1135
1118, Second Electron Injection
1114, First Electron Injection
1112, End of Flux Decrease
Geosynchronous Events

Figure 10

Sketch of Multiple Plasmoid Formation

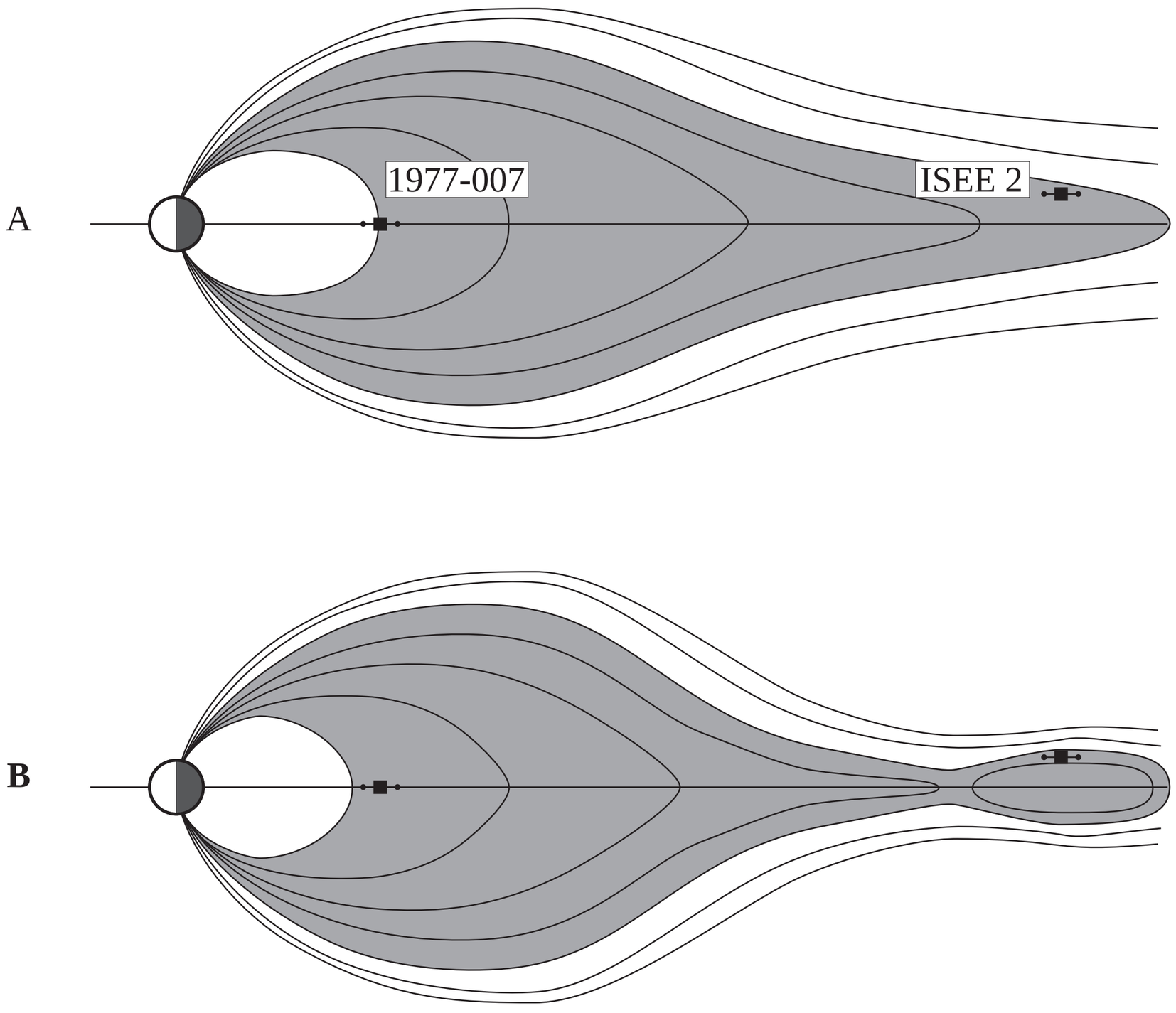

Figure 11

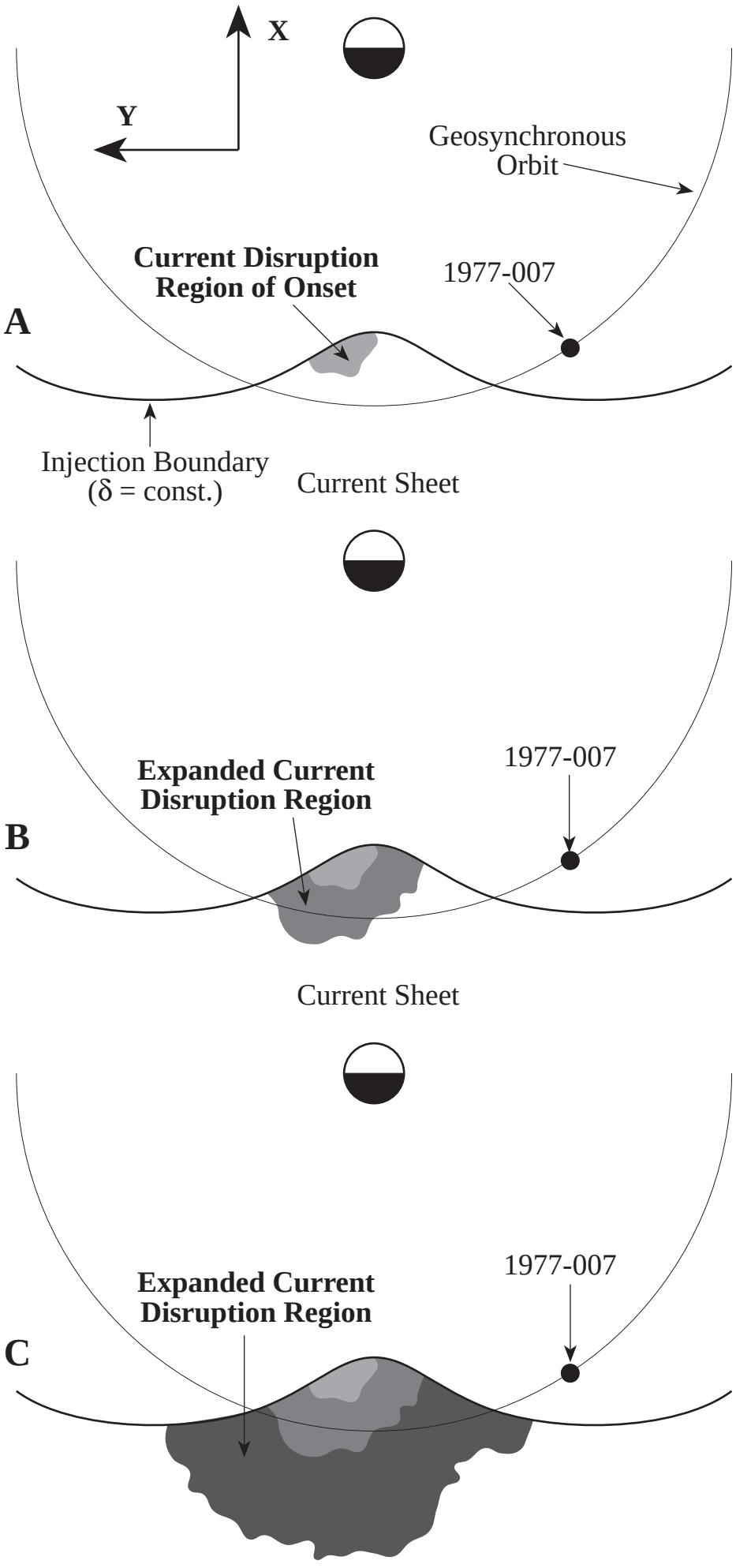
X
Y
Geosynchronous
Orbit
Current Disruption
Region of Onset
1977-007
A
Injection Boundary
(δ = const.)
Current Sheet
Expanded Current
Disruption Region
1977-007
B
Current Sheet
Expanded Current
Disruption Region
1977-007
C

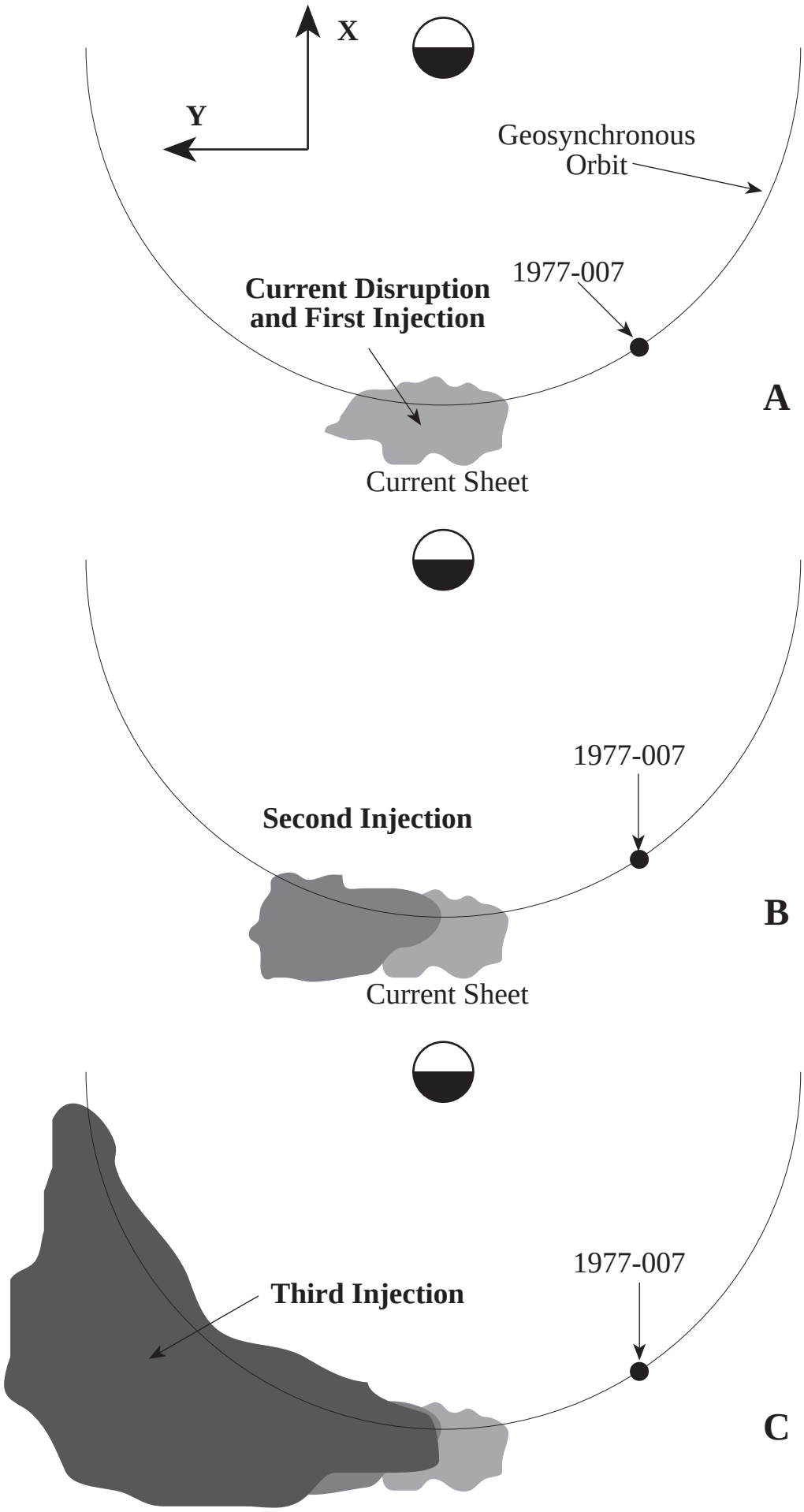
X
Y
Geosynchronous
Orbit
1977-007
Current Disruption
and First Injection
A
Current Sheet
1977-007
Second Injection
B
Current Sheet
1977-007
Third Injection
C